Stanford Exploration Project, Report 97, July 8, 1998, pages 117–131

Stanford Exploration Project, Report 97, July 8, 1998, pages 117–131

Discrete Kirchhoff theory and irregular geometry

Nizar Chemingui and Biondo Biondi[1]

keywords: *Kirchhoff, AMO, inverse, adjoint, scaling, normalization, interpolation, inversion, preconditioning, regularization*

ABSTRACT

Discrete implementations of integral operators are essentially matrix-vector multiplications. In this paper, we study the structure of Kirchhoff-type matrices where each row corresponds to a summation surface and each column corresponds to an impulse response. Due to irregularities in seismic coverage, the columns and rows are generally badly scaled. To balance the coefficients of the matrix, we propose two formulations for normalization: a data-space formulation based on row scaling of pull (sum) operators, and a model-space normalization based on column scaling of push (spray) operators. In both approaches, the final image is normalized by a reference model that is the operator's response to an input vector with all components equal to one. We apply this normalization technique to approximate a data covariance matrix based on the definition of a data-space pseudo inverse. This data covariance is an AMO matrix. It represents an equalization filter that corrects the imaging operator for the interdependencies among data parameters. We investigate the use of the normalization operators as preconditioners for the iterative solution of multichannel inversion. The diagonal transformation ensures common magnitude to all the variables and accelerates the convergence of the linear solver. Beyond the goal of fold normalization, the advantage of the iterative solution is to interpolate for missing data and reduce the artifacts related to data aliasing.

INTRODUCTION

Kirchhoff imaging techniques have been widely used on 3D datasets since they can be applied to any subset of the full prestack data and, presumably, can handle irregular geometry. Mathematical derivations of integral operators assume continuous wavefields. In practice, the resulting imaging algorithms are only applied to discretely sampled seismic data and their implementations simply reduce to a matrix-vector multiplication. Due to irregular coverage, the matrix is ill-conditioned and the linear systems that need to be solved may be badly scaled. It is therefore advisable to

[1] **email:** nizar@sep.stanford.edu,biondo@sep.stanford.edu

normalize the discrete summations (Beasley and Klotz, 1992; Ronen, 1994).

Chemingui and Biondi (1996) proposed a simple technique to compensate for the effects of irregular fold distributions. The method extends the multiplicity concept in CMP stacking to wave equation processes. It normalizes each input trace in the prestack process according to the local stacking fold of its corresponding bin. The technique has the advantage of being independent of the imaging operator and depends only on the acquisition geometry. However, it cannot account for the time and space variability of the operators, their limited aperture, or for varying velocity functions. In this paper we propose two alternative approaches for fold normalization depending on the numerical implementation of the algorithms. We relate the weights to the concept of "fold" in Kirchhoff imaging and show that the technique is essentially equivalent to calibrating the image by the response of a flat event.

Based on the definition of data-space pseudo inverse (Chemingui and Biondi, 1997c), we apply the normalization technique to estimate an inverse for the cross-product operator in the two-step solution of Chemingui and Biondi (Chemingui and Biondi, 1997a). The approximate solution enables an efficient computation for a data covariance matrix, and thus, for the fold equalization problem. This covariance matrix corrects the imaging operator for interdependencies between data-elements. It is computationally more attractive than the numerical solution based on iterative solvers.

To go beyond the normalized pseudo inverse, we can use the diagonal transformation as a preconditioner for iterative solutions. Chemingui and Biondi (1997) presented an inversion technique that is suitable for sparse and uneven sampling and takes advantage of the abundance of seismic traces in multifold seismic data to interpolate beyond aliasing. The technique, which we now refer to as *Inversion to Common Offset (ICO)*, is based on least-squares theory and wave-equation interpolation for missing data using the azimuth-moveout operator (Biondi and Chemingui, 1994). To guide the iterative optimization to the desired solution, we precondition the inversion by the normalization operator. The diagonal transformation proves to be a suitable preconditioner for the dealiasing inversion.

In this paper we first discuss discrete Kirchhoff methods and their associated algorithms. We relate the implementations to the concepts of accuracy of operators and proper handling of the irregular geometry in true-amplitude imaging. Next we present the two formulations for column and row normalization which we refer to as data and model normalization. Finally we demonstrate the efficiency of the diagonal transformation for normalizing the fold, providing better approximation of a pseudo-inverse and defining an operator that is as unitary as possible and well preconditioned for linear solvers.

DISCRETE KIRCHHOFF IMPLEMENTATIONS

Kirchhoff operators represent a class of linear operators based on integral solutions to the wave equation. The linearity of the transformation follows from the linear properties of integrals. The implementation of integrals as discrete summation reduces to matrix-vector multiplication where we hardly ever write down these matrices. The linear operation transforms a space to another space (e.g., a data space $\mathbf{d}$ to a model space $\mathbf{m}$). These spaces are simply represented by vectors whose components are packed with numbers. The relation between data and model is then represented by the linear system of equations:

$$\mathbf{d} = \mathbf{L}\mathbf{m}. \tag{1}$$

This is often referred to as the forward modeling relation, where the goal of imaging is to perform the inverse of these calculations, i.e., to find models from the data. Mathematically, this is equivalent to estimating the inverse of the operator $\mathbf{L}$.

True-amplitude imaging

With the forward modeling relation in mind, it is possible for many processes to derive an analytical formulation for the inverse of the modeling operator. Whenever an exact formulation of the imaging operator is obtainable, it is referred to as an amplitude-preserving transformation. A considerable volume of literature establishes theory for deriving the inverse based on asymptotic theory for Kirchhoff modeling and Born scattering. The resulting algorithms are then applied to discrete seismic data through the linear transformation

$$\mathbf{m} = \mathbf{F}\mathbf{d}. \tag{2}$$

True amplitude imaging aims at deriving the proper weights along the summation surfaces or impulse responses of $\mathbf{F}$. A well studied example is the case of the migration operator. Jaramillo and Bleistein (1997) derived amplitude-preserving weights for migration and demigration based on the Kirchhoff modeling formula. Then based on the superposition principle they derived two alternative operators to perform migration as isochron superposition and demigration as diffraction superposition. We find the two concepts rather easier to understand using Claerbout's terminology for push and pull operators defined below.

Push and Pull operators

Jon Claerbout (1998) writes: "*The simplest and most fundamental linear operators arise when a matrix operator reduces to a simple row or column.*" A row is a summation operation and a column is an impulse response. If the inner loop of a matrix-multiply ranges within a *row*, the operator is called *sum* or *pull*. If the inner loop ranges within a *column*, the operator is called *spray* or *push*.

KIRCHHOFF IMAGING AND IRREGULAR GEOMETRY

For idealized geometry, the previous analysis could ensure amplitude-preserved operators and well behaved matrices. Problems arise in 3D multichannel recording where the reality of seismic acquisition causes seismic data to be sampled in a sparse and irregular fashion. These irregularities are often observed in the form of variations in fold coverage resulting in an abundance of seismic traces in some bins and missing data in others.

Considering an imaging operator $\mathbf{F}$ (for instance $\mathbf{F} = \mathbf{L^{-1}}$), each row of $\mathbf{F}$ corresponds to an output bin and each column corresponds to a data trace. Due to the irregular coverage, the columns and rows of $\mathbf{F}$ are badly scaled and the matrix is ill-conditioned. Its condition can be improved by column scaling (Ronen, 1994).

Based on a similar approach, we propose two formulations for row and column normalization which we refer to as *image normalization* and *data normalization*. They involve pre- and post-multiplying the operator $\mathbf{F}$ by a diagonal matrix whose diagonal entries are the inverse of the sum of the rows or columns of $\mathbf{F}$.

Since Kirchhoff operators are associated with matrices that contain no negative elements, it is safe to use the sum of the elements. In case of negative entry values, we can sum the absolute values of the elements or compute the norms of the rows or columns. Similarly for the case of complex values, we should use an L_2 norm to compute the diagonal entries of the normalization operator; i.e., the square root of the sum of elements squared.

Row scaling: model normalization

Since each row corresponds to a summation surface, we apply the row normalization to imaging operators implemented as (sum) pull operators. We solve the normalized system:

$$\mathbf{m} = \mathbf{R}^{-1}\mathbf{F}\mathbf{d} \tag{3}$$

where the sum of the elements of each row is along the diagonal of $\mathbf{R}$.

The solution in (3) is equivalent to applying the imaging operator $\mathbf{F}$ followed by a diagonal transformation $\mathbf{R^{-1}}$. Therefore, we will refer to this normalization as model or *image normalization*. Since $\mathbf{R^{-1}}$ has the inverse units of $\mathbf{F}$, the normalized image is unit-less.

Given that each row of $\mathbf{F}$ corresponds to an output bin, $\mathbf{R^{-1}}$ is therefore normalization by the coverage after imaging. We refer to this coverage as the *imaging fold*, e.g, AMO fold, DMO fold ... etc.

Column scaling: data normalization

Recall that each column of $\mathbf{F}$ corresponds to an impulse response. We therefore apply column scaling to imaging operators implemented as push operators. The system we solve is then

$$\mathbf{m} = \mathbf{F}\mathbf{C}^{-1}\mathbf{d}, \tag{4}$$

where the sum of the elements of each column are on the diagonal of $\mathbf{C}$.

In equation (4) the imaging operator is applied after the data have been normalized by $\mathbf{C^{-1}}$ and, consequently, we will refer to this normalization as *data normalization*. Again we notice that $\mathbf{C^{-1}}$ has the inverse units of $\mathbf{F}$ making the output image unit-less.

Similarly to the imaging fold defined earlier, $\mathbf{C^{-1}}$ is normalization by the coverage of the modeling operator $\mathbf{L}$ (where $\mathbf{F} = \mathbf{L^{-1}}$). We will refer to this coverage as the *modeling fold*.

Normalizing vs scaling of the adjoint

Imaging is quite often derived as the adjoint of modeling, where in the absence of explicit formulation for $\mathbf{F}$ we seek an approximate inverse for $\mathbf{L}$. Mathematically, this means that we approximate an inverse of a matrix of very high order by the transpose (Hilbert adjoint) of $\mathbf{L}$.

Claerbout (1998) points out that unless $\mathbf{L}$ has no physical units, the units of the transpose solution $\mathbf{m_t} = \mathbf{L^T d}$ do not match those of $\mathbf{m_t} = \mathbf{Fd}$. Given the theoretical (least squares) solution $\mathbf{m_{lsq}} = (\mathbf{LL^T})^{-1}\mathbf{F^T d}$, Claerbout suggests that the scaling units should be those of $(\mathbf{LL^T})^{-1}$. He proposes a diagonal weighting function suggested by Bill Symes (private communication) that makes the image $\mathbf{m_t} = \mathbf{W^2 L^T d}$, where we chose the weighting function to be

$$\mathbf{W}^2 = \mathbf{diag}\left(\frac{\mathbf{L}^T\mathbf{d}}{\mathbf{L}^T\mathbf{L}\mathbf{L}^T\mathbf{d}}\right), \tag{5}$$

which obviously has the correct physical units.

Comparing the normalized solution to the scaled adjoint, we see that the normalized solution is unit-less. It therefore avoids the ambiguity in guessing approximate weights. The normalized solution represents a ratio of two images where the reference image is the output of an input vector with all components being equal to one. This is equivalent to a calibration by a flat event response. Similar approaches might exist in practice some of them derived in heuristic ways, e.g., the DMO fold (Slawson et al., 1995).

The normalization technique can also be applied to approximate inverses; i.e., to the adjoint. The normalized solution is again unit-less and represents a ratio of two approximate images. This will not make the final image exact, but, similarly to the case of normalized inverse, it calibrates the data for the effects of varying fold. In the next section we show how we can apply this concept to better approximate a pseudo-inverse and estimate a data covariance matrix.

TWO-STEP SOLUTION FOR FOLD EQUALIZATION

Using the definition of data-space pseudo inverse, Chemingui and Biondi (1997) presented a new technique to invert for reflectivity models while correcting for the effects of irregular sampling. The final reflectivity model is a two step solution where the data is equalized in a first stage with an inverse filter and an imaging operator is then applied to the equalized data to invert for a model.

We start from the definition for the data-space inverse solution

$$\mathbf{m} = \mathbf{L}^T(\mathbf{L}\mathbf{L}^T)^{-1}\mathbf{d}, \tag{6}$$

then considering an irregularly sampled input of n seismic traces and letting $\mathbf{L_{m,d_i}}$ be the operator that maps trace d_i into the model space $\mathbf{m}$, we write the cross-product matrix $\mathbf{LL^T}$ as

$$\mathbf{LL^T} = \begin{bmatrix} \left[\mathbf{L_{(m,d_1)}L^T_{(m,d_1)}}\right] & \left[\mathbf{L_{(m,d_1)}L^T_{(m,d_2)}}\right] & \cdots\cdots & \left[\mathbf{L_{(m,d_1)}L^T_{(m,d_n)}}\right] \\ \left[\mathbf{L_{(m,d_2)}L^T_{(m,d_1)}}\right] & \left[\mathbf{L_{(m,d_2)}L^T_{(m,d_2)}}\right] & \cdots\cdots & \left[\mathbf{L_{(m,d_2)}L^T_{(m,d_n)}}\right] \\ . & . & . & . \\ . & . & . & . \\ . & . & . & . \\ \left[\mathbf{L_{(m,d_n)}L^T_{(m,d_1)}}\right] & \left[\mathbf{L_{(m,d_n)}L^T_{(m,d_2)}}\right] & \cdots\cdots & \left[\mathbf{L_{(m,d_n)}L^T_{(m,d_n)}}\right] \end{bmatrix} \tag{7}$$

Each inner product $\left[\mathbf{L_{(m,d_i)}L^T_{(m,d_j)}}\right]$ is therefore a reconstruction of a data trace with input offset h_i as a new trace with offset h_j. We recognize this mapping as an AMO transformation. We name this cross product filter $\mathbf{A}$, and we write it in terms of its AMO elements as

$$\mathbf{A} = \begin{bmatrix} \mathbf{I} & \mathbf{A_{(h_1,h_2)}} & \mathbf{A_{(h_1,h_3)}} & \cdots & \mathbf{A_{(h_1,h_n)}} \\ \mathbf{A_{(h_2,h_1)}} & \mathbf{I} & \mathbf{A_{(h_2,h_3)}} & \cdots & \mathbf{A_{(h_2,h_n)}} \\ \mathbf{A_{(h_3,h_1)}} & \mathbf{A_{(h_3,h_2)}} & \mathbf{I} & \cdots & \mathbf{A_{(h_3,h_n)}} \\ . & . & . & . & . \\ . & . & . & . & . \\ . & . & . & . & . \\ \mathbf{A_{(h_n,h_1)}} & \mathbf{A_{(h_n,h_2)}} & \mathbf{A_{(h_n,h_3)}} & \cdots & \mathbf{I} \end{bmatrix} \tag{8}$$

where $\mathbf{A_{(h_i,h_j)}}$ is AMO from input offset h_i to output offset h_j and, $\mathbf{I}$ is the identity operator (mapping from h_i to h_i). Conforming to the definition of AMO (Biondi et al., 1996), $\mathbf{A_{(h_i,h_j)}}$ is the adjoint of $\mathbf{A_{(h_j,h_i)}}$; therefore, the filter $\mathbf{A}$ is Hermitian with diagonal elements being the identity and off-diagonal elements being AMO transforms.

Two-step solution

The fundamental definition of $\mathbf{A}$ from equation (7) allows analytic computations of its inner product elements. The challenge is then to solve for the inverse of $\mathbf{A}$. First, we write the solution for $\mathbf{m}$ from equation (6) in terms of $\mathbf{A}$ as

$$\mathbf{m} = \mathbf{L^T A^{-1} d}. \tag{9}$$

Then we change the data variable $\mathbf{d}$ to a new variable $\hat{\mathbf{d}}$ and recast the problem as

$$\mathbf{m} = \mathbf{L^T} \hat{\mathbf{d}} \tag{10}$$

where $\hat{\mathbf{d}}$ is the filtered input given by the substitution:

$$\hat{\mathbf{d}} = \mathbf{A^{-1} d} \tag{11}$$

Solving for $\hat{\mathbf{d}}$, we then need to compute the inverse of $\mathbf{A}$. This is essentially the first step of the solution, i.e., the data-equalization step. After filtering, we merely need to apply the imaging operator to the equalized data to obtain the final image. At this stage, any true-amplitude imaging process could be applied, e.g., prestack Kirchhoff migration.

Estimating the data covariance

If we change sides in equation (11) and rewrite it in the more standard form:

$$\mathbf{d} = \mathbf{A} \hat{\mathbf{d}}, \tag{12}$$

then equation (12) looks similar to the linear relation (1) that relates a data vector to a model. Given that $\mathbf{A}$ is essentially an AMO matrix, then all its elements are positive. This is also evident since $\mathbf{A}$ represents a cross product matrix.

To estimate an approximate inverse for $\mathbf{A}$ we apply the same normalization techniques in computing its inner product entries, which are, AMO transformation from a given input geometry to another. This normalization makes the cross-product matrix unit-less. Therefore when approximating $\mathbf{A^{-1}}$ by its transpose we avoid the ambiguity of scaling this adjoint. Moreover, since $\mathbf{A}$ is hermitian, then it is equal to its transpose.

We conclude that $\mathbf{A}$ is itself a data covariance matrix. It represents an equalization filter that measures the interdependencies among the data elements and corrects the imaging operator for the effects of fold variations.

INVERSION TO COMMON OFFSET

Inversion to common offset (Chemingui and Biondi, 1997b) is an accurate but costly technique for processing irregularly sampled 3D data. The inversion is not restricted to zero offset models or to a particular azimuth. The model, in general, simulates a regular common-offset experiment. For practical 3D applications, we use a cost-effective implementation based on a log-stretch transformation (Bolondi et al., 1982), after which AMO becomes time invariant and the inversion can be split into independent frequencies. The linear inverse problem we solve for each frequency component can be written as:

$$\mathbf{d} = \mathbf{L}\mathbf{m}, \tag{13}$$

where the vector $\mathbf{d}$ represents the irregular input data, $\mathbf{L}$ represents the modeling operator, and $\mathbf{m}$ stands for the regularly sampled model.

Diagonal weighting preconditioning

In the inversion relation (13), the number of equations is the number of traces in the input data and the number of unknowns is the number of output traces or bins. Since $\mathbf{L}$ is unbalanced, we can improve its condition by diagonal weighting (Ronen, 1994). We apply the row and column normalization operators described earlier as preconditioners. Similar approaches based on diagonal scaling are discussed in the mathematical literature using different norms for the columns. Often they are referred to as left and right preconditioners; we prefer to call them *data-space* and *model-space* preconditioners. The rationale in the terminology is based on the fact that the scaled adjoint is the first step of the inversion. With left preconditioning the adjoint operator is applied after the data have been normalized by the diagonal operator. We therefore refer to this solution as *data-space* preconditioning. Right preconditioning is equivalent to applying the adjoint operator $\mathbf{L}^T$ followed by a scaling of the model by the diagonal operator. Consequently, we refer to this approach as *model-space* preconditioning.

Data-space preconditioning

This is equivalent to pre-multiplying $\mathbf{L}$ by the diagonal matrix $\mathbf{R^{-1}}$ and solving the system:

$$\mathbf{R}^{-1}\mathbf{d} = \mathbf{R}^{-1}\mathbf{L}\mathbf{m} \tag{14}$$

The data-space preconditioner can be interpreted as an approximation to a "data covariance" operator that is used to express the reliability and the correlation of the data measurements. In iteratively re-weighted least squares, it approximates a data variance measure that can be estimated from the current residual (Nichols, 1994).

Model-space preconditioning

The technique is based on a post-multiplication of the matrix $\mathbf{L}$ by the diagonal matrix $\mathbf{C^{-1}}$. The preconditioning operator introduces a new model $\mathbf{x}$ given by

$$\mathbf{x} = \mathbf{Cm} \tag{15}$$

By the preconditioning transformation, we have recast the original inversion relation (13) into

$$\mathbf{d} = \mathbf{LC}^{-1}\mathbf{x}. \tag{16}$$

After solving for $\mathbf{x}$ we easily compute $\mathbf{m} = \mathbf{C}^{-1}\mathbf{x}$.

SYNTHETIC EXAMPLE

In this section we present simple examples of discrete Kirchhoff implementations as matrix-vector multiplication on irregularly sampled data. The experiments were designed to illustrate several approaches for efficient handling of irregular geometry: (a) by normalized imaging, (b) by two step equalization and (c) by Inversion to Common Offset (ICO). The implementations are all done in the $(\omega, x, y))$ domain for comparison with the ICO results.

We use the fold distribution shown in Figure 1. The fold chart represents a subset from a real 3-D land survey. We extracted the header values of traces whose source-receiver azimuth is between -30^o and 30^o with an absolute-offset range from 1000 to 1200 m. The reflectivity model consists of a single dipping bed with a strike of 60^o from the inline direction. A monochromatic planewave is used to create the synthetic input data, and therefore, only one frequency slice is processed. All the results are displayed in the Fourier domain of the log-stretched data. We analyze the effects of fold variations on the imaginary part of the wavefield.

In the first experiment, the model is a common-offset section of 50 by 50 CMP's with 35m spacing. This is the nominal CMP spacing of the real survey. The second panel in Figure 1 shows the ideal result from a synthetic experiment which simulates zero-azimuth acquisition and a constant offset of 1100 m. This is the unknown model that solves the set of equations in (13). The bottom two panels are the results of processing with true-amplitude AMO (Chemingui and Biondi, 1995). The effects of varying fold are noticeable on the un-normalized image. In absence of empty bins there are no aliasing artifacts other than amplitude distortions. The result of normalized AMO is nearly perfect on this low frequency model.

The challenging task in handling irregular sampling is dealing with aliasing which is a missing data problem. In the second experiment we used the same subset of traces and created a zone of missing coverage by removing traces over some large area. The size of the uncovered area is about 8 bins in both the inline and crossline directions. We also used a higher frequency to simulate the response of the steeply dipping bed. We chose a model resolution of 17.5 m which corresponds to half the nominal CMP-spacing of the data.

Figure 2 shows the results of processing with AMO. These are the outputs of applying AMO to reconstruct the data with zero common-azimuth and 1100-m effective offset. The result of un-normalized AMO displays poor quality in the area of missing coverage. As result of the normalization, the interpolated values for the missing data are calibrated on the normalized image and result into better resolution. Some aliasing artifacts are still noticeable and are due to the limited interpolation by AMO. As in the previous experiment, fold variations in form of trace redundancy were properly handled by the diagonal normalization.

The result of the two-step solution (equalization with a data covariance operator + imaging with AMO) is shown in Figure 3. We compare it to the output of ICO with and without preconditioning. After 5 iterations with a conjugate gradient solver the preconditioned inversion yielded a reasonably good solution where the solution without preconditioning is still far from convergence.

Overall, the preconditioned ICO yielded the best picture in terms of fold equalization and dealiasing. The two step solution, with explicit analytic computation of the data covariance operator, presented a good and cost effective solution to the problem of irregular sampling. This is an important result considering the alternative cost of estimating the equalization filter numerically using iterative solvers. The normalized one step imaging is still an attractive approach given that it can greatly eliminate the effects of fold variations at only twice the cost of conventional imaging.

CONCLUSIONS

We have presented new developments for accurate implementations of discrete Kirchhoff operators as matrix-vector multiplication. The main process is based on the normalization of the Kirchhoff matrix by a diagonal transformation using the sum of the rows (summation surfaces) and columns (impulse responses). The normalization operator is designed in consistency with the numerical implementation of the Kirchhoff operator as pull (sum) or push (spray) operator. The final image is normalized by a reference model that is the operator's response to an input vector with all components equal to one (flat event).

We also presented an explicit formulation of a data covariance matrix for the solution of two-step inversion of irregularly sampled data. This data covariance is an AMO matrix that measures the correlations among data elements and corrects the imaging operator for the effects of irregular sampling.

Beyond the fold normalization, the diagonal transformations have proved to be a suitable preconditioner for the Inversion to Common Offset (ICO). It accelerates the convergence of the iterative solution and, therefore, enables a cost effective technique for 3D dealiasing inversion.

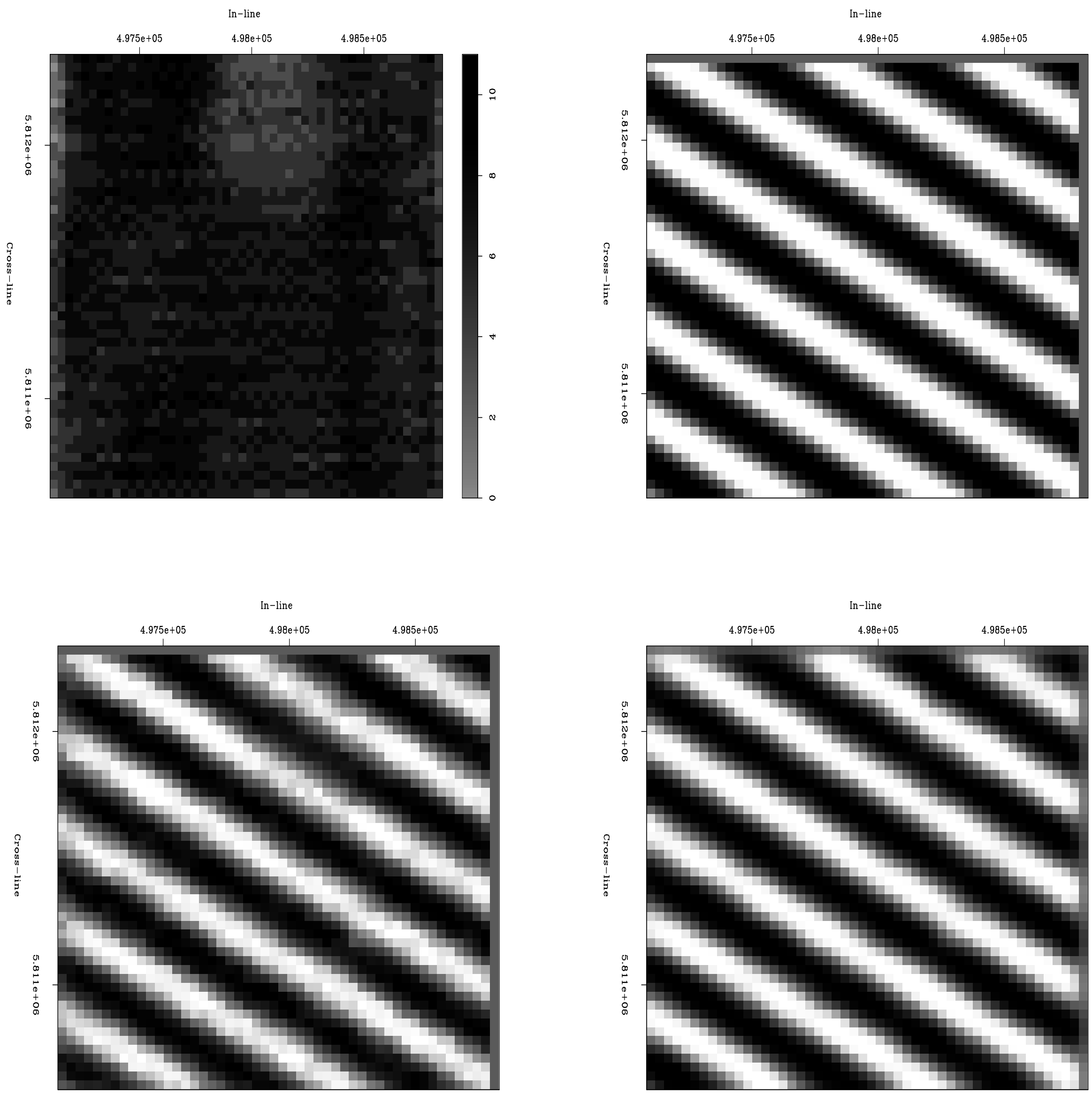

Figure 1: (top left) Fold distribution of the input data with offset range between 1000 m and 1200 m and azimuth range between -30 and 30 degrees; (top right) Ideal synthetic model: Log stretch Fourier domain response of a dipping bed to a monochromatic wavefront; (bottom left) Un-normalized AMO stack at zero azimuth and 1100 m offset.; (bottom right) Normalized AMO stack. $\boxed{\text{nizar1-figure1}}$ [CR]

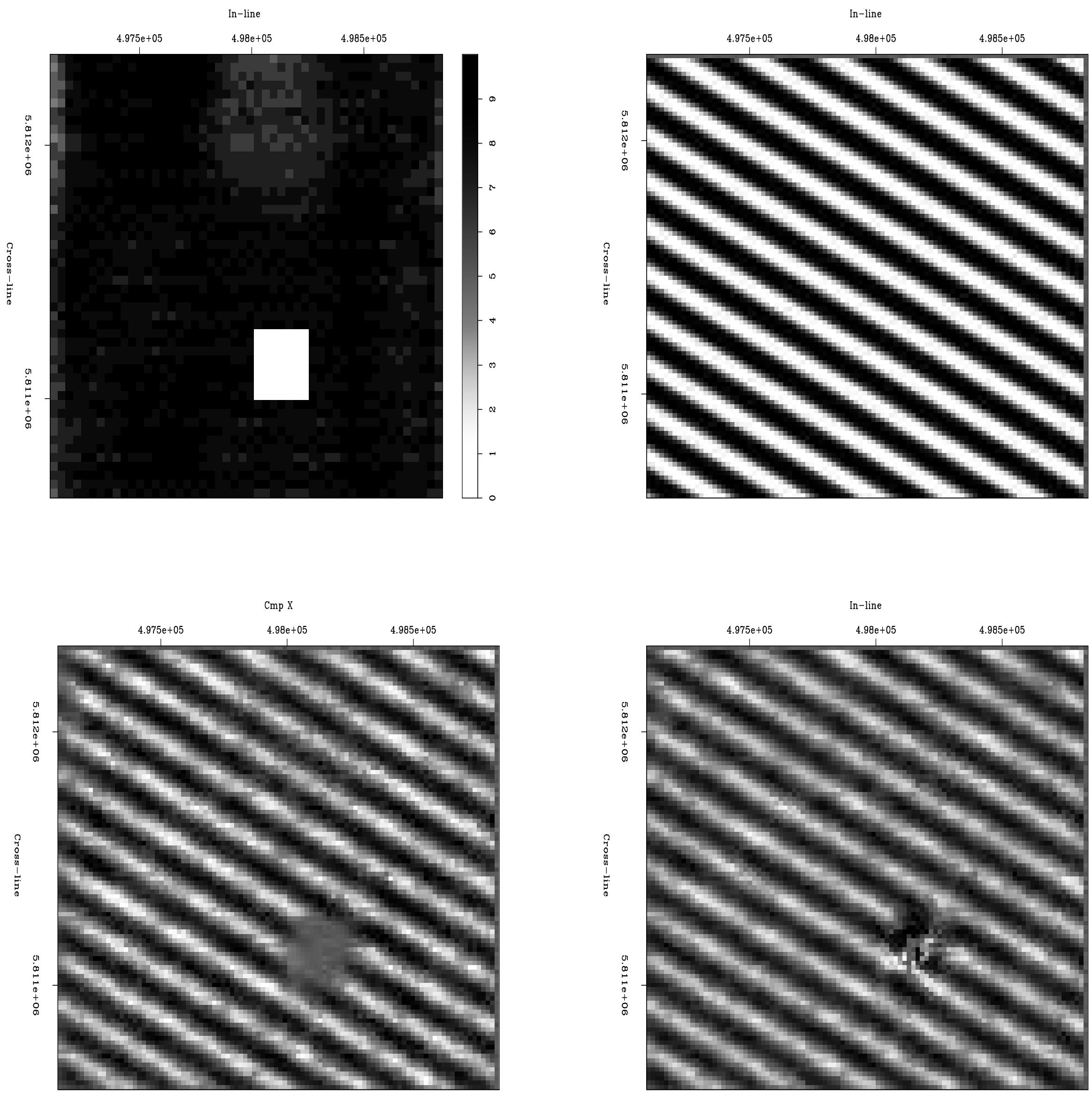

Figure 2: (top left) Fold chart of input data with missing coverage; (top right) Ideal synthetic model: response of a dipping event using higher frequency and ideal recording geometry of zero azimuth and 1100 m offset; (bottom left) Un-normalized AMO stack at zero azimuth and 1100 m offset; (bottom right) Normalized AMO stack. nizar1-figure2 [CR]

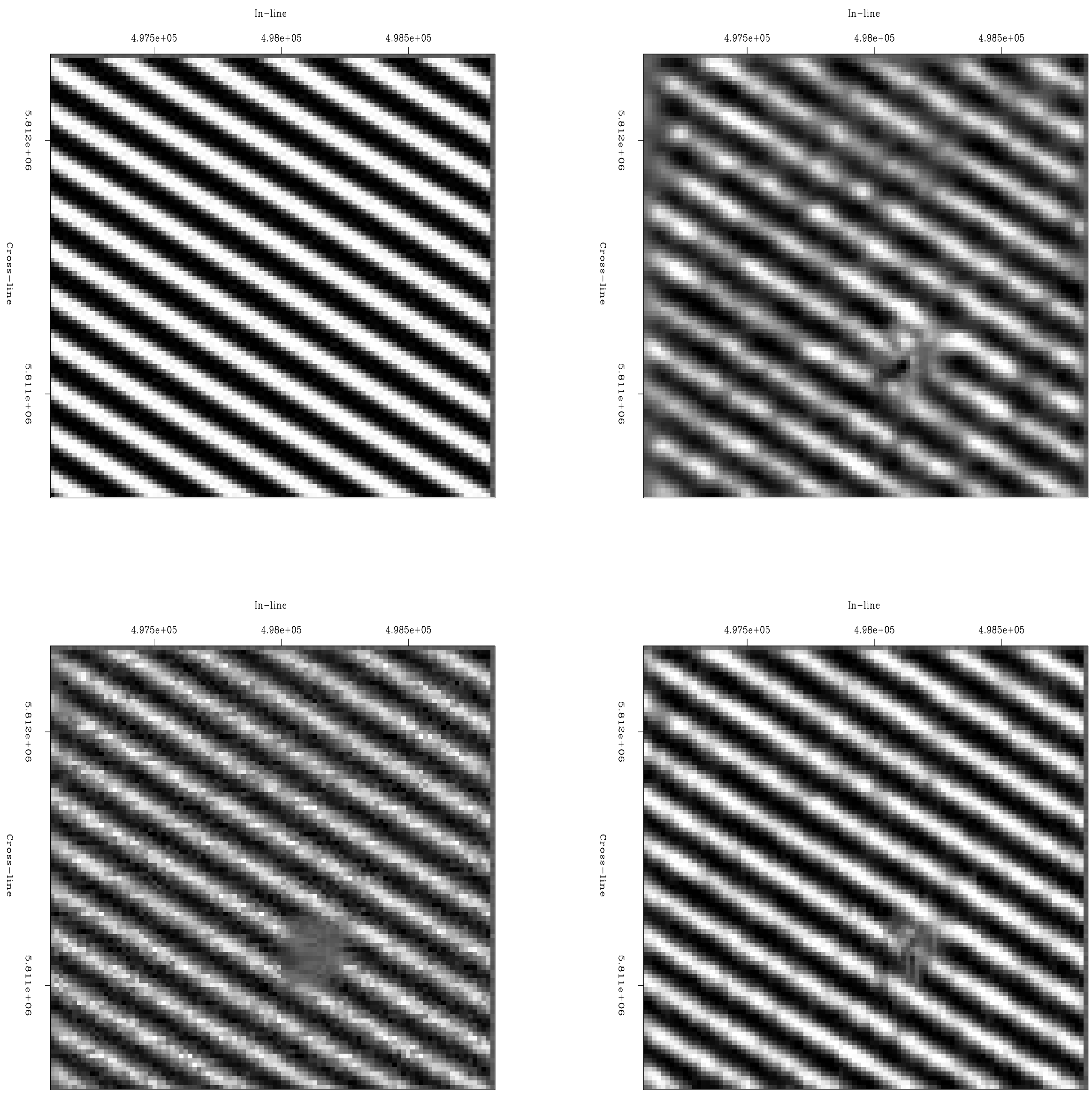

Figure 3: (top left) Ideal model; (top right) Two-step solution: equalization with a data covariance operator then AMO transformation to zero azimuth and 1100 m offset; (bottom left) Inversion result without preconditioning after 5 iterations of CG; (bottom right) Preconditioned ICO after 5 iterations of CG nizar1-figure3 [CR]

REFERENCES

Beasley, C. J., and Klotz, R., 1992, Equalization of DMO for irregular spatial sampling: 62nd Annual Internat. Mtg., Soc. Expl. Geophys., Expanded Abstract s, 970–973.

Biondi, B., and Chemingui, N., 1994, Transformation of 3-D prestack data by Azimuth Moveout: SEP–**80**, 125–143.

Biondi, B., Fomel, S., and Chemingui, N., 1996, Azimuth moveout for 3-D prestack imaging: Geophysics, accepted for publication.

Bolondi, G., Loinger, E., and Rocca, F., 1982, Offset continuation of seismic sections: Geophys. Prosp., **30**, no. 6, 813–828.

Chemingui, N., and Biondi, B., 1995, Amplitude-preserving azimuth moveout: Expanded Abstracts, 1453–1456.

Chemingui, N., and Biondi, B., 1996, Normalization of Kirchhoff imaging for variable fold: SEP–**93**, 51–62.

Chemingui, N., and Biondi, B., 1997a, Equalization of irregular data by iterative inversion: Expanded Abstracts, 1115–1118.

Chemingui, N., and Biondi, B., 1997b, On the inversion of 3D multichannel data: SEP–**95**, 227–237.

Chemingui, N., and Biondi, B., 1997c, Two-step inversion of irregular data: SEP–**94**, 91–107.

Claerbout, J. Geophysical Estimation by Example: Environmental soundings image enhancement:. http://sepwww.stanford.edu/sep/prof/, 1998.

Jaramillo, H. H., and Bleistein, N., 1997, Demigration and migration in isotropic inhomogeneous media: 67th Annual Internat. Mtg., Soc. Expl. Geophys., Expanded Abstracts, 1673–1676.

Nichols, D., 1994, A simple example of a null space and how to modify it: SEP–**82**, 177–182.

Ronen, S., 1994, Handling irregular geometry: Equalized DMO and beyond: 64th Ann. Internat. Meeting, Soc. Expl. Geophys., Expanded Abstracts, 1545–1548.

Slawson, S. E., Monk, D. J., and Sudhakar, V., 1995, DMO implications for 3-D survey design: 65th Annual Internat. Mtg., Soc. Expl. Geophys., Expanded Abstracts, 935–938.